Structure of Atactic Polystyrene: A Molecular Dynamics Simulation Study

Chakravarthy Ayyagari, Dmitry Bedrov, and Grant D. Smith*

Department of Chemical and Fuels Engineering and Department of Materials Science and Engineering, 122 S. Central Campus Drive Rm. 304, University of Utah, Salt Lake City, Utah 84112

Received February 28, 2000; Revised Manuscript Received June 6, 2000

ABSTRACT: We have performed a molecular dynamics simulation study of atactic polystyrene (a-PS) and its dimer 2,4-diphenylpentane (DPP) using a previously derived quantum chemistry based explicit atom force field. The X-ray structure factor of a-PS obtained from simulations was found to be in good agreement with experiment, reproducing the "amorphous" peak at around 1.4 $Å^{-1}$ as well as the "polymerization peak" at around 0.75 $Å^{-1}$ and its anomalous temperature dependence (increasing intensity with increasing temperature). We found that the amorphous peak in a-PS arises primarily from phenyl−phenyl correlations, with important intramolecular and intermolecular contributions. While the intermolecular component was found to shift to lower q with increasing temperature, the intramolecular component was found to be insensitive to temperature, resulting in a weak temperature dependence of the amorphous peak. Simulations revealed the presence of the polymerization peak in DPP, indicating that the designation "polymerization peak" for this feature is a misnomer. The polymerization peak in both a-PS and DPP was found to be due primarily to intermolecular correlations of backbone atoms. This underlying correlation showed the expected decrease in intensity and shifting to lower q with increasing temperature. The shifting to lower q of intermolecular phenyl−phenyl and phenyl−backbone correlations with increasing temperature was found to lead to the observed anomalous temperature dependence of the polymerization peak.

I. Introduction

One of the most intriguing features of polystyrene is the so-called "polymerization peak" in its wide-angle X-ray structure factor.[1−4] The X-ray scattering pattern of atactic polystyrene (a-PS) reveals a diffuse halo (polymerization peak) at around $q = 0.75$ A^{-1} in addition to a higher q feature at around 1.4 $Å^{-1}$ associated with the ubiquitous "amorphous halo" observed in polymer melts, glasses, and rubbers, as illustrated in Figure 1. The polymerization peak was first reported by Katz[1] in 1927. He confirmed the presence of similar peaks in other polymers such as polyindine and polycumarone. The peak has also been observed in quenched isotactic polystyrene.[3] X-ray patterns of most polymer glasses, rubbers, and melts do not exhibit such a peak. The feature is also absent in scattering patterns of the styrene monomer as well as liquid benzene. The temperature dependence of this peak exhibits anomalous behavior in that the intensity of the peak increases with increasing temperature, apparently indicating enhanced structure at higher temperatures.

Although a-PS has been studied extensively for several decades, the origin of the polymerization peak is not well understood. The observation that the polymerization peak increases in intensity on the equator, i.e., normal to the extension axis, under plastic extension[3] indicates an important intermolecular contribution. As increasing thermal disorder with increasing temperature is expected to reduce intermolecular correlations, any explanation for the polymerization peak must account for changes in structure with increasing temperature that override these effects. We believe that molecular dynamics (MD) simulations can play an important role in helping understand the structure of a-PS. While several MD simulations of a-PS investigating structure have been performed using both all-atom[5] and united-atom[5,6] potential functions, a detailed analysis of the polymerization peak has not been conducted. Simulations that are of sufficient accuracy to help develop a detailed picture of the structure of a-PS

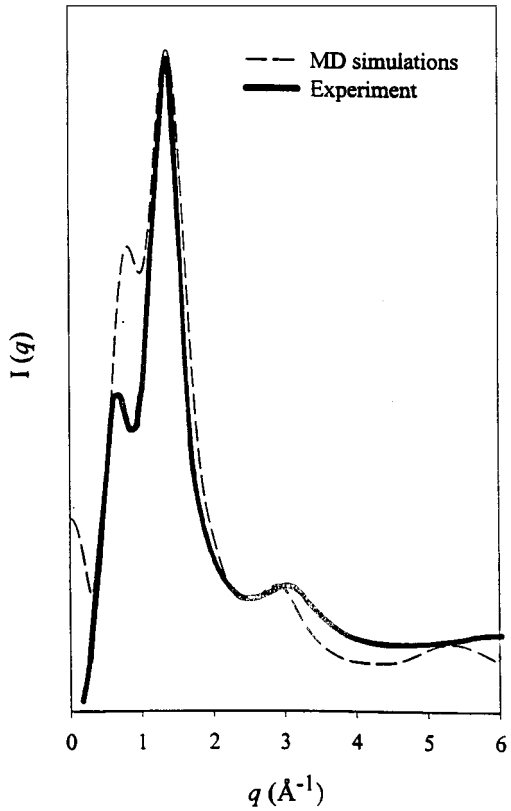

Figure 1. X-ray scattering intensity for atactic polystyrene from experiment[2] (293 K, solid line) and molecular dynamics simulation (298 K, dashed line).

10.1021/ma0003553 CCC: $19.00
Published on Web 07/21/2000

require a model that reproduces the complex conformational characteristics of the polymer and accurately describes intermolecular interactions. We have developed an all-atom potential for polystyrene and its oligomers based upon high-level quantum chemistry calculations on benzene dimer[7,8] and 1,2-diphenylpentane (DPP).[9] Here, we report on the structure of a-PS, meso DPP (m-DPP), and racemic DPP (r-DPP) as determined from MD simulations using the quantum chemistry based potential function, with emphasis on the origin of the polymerization peak and its temperature dependence.

II. Simulation Methodology

Molecular dynamics simulations were performed on 16 chains of polystyrene each of 21 repeat units (MW = 2200) at 298, 400, and 450 K. Alternate carbons in the backbone are chiral centers with side groups placed randomly to yield a dyad replication probability of 0.5. Initially, the chains were arranged on a low-density lattice. Stochastic dynamics[10] were performed at elevated temperature and reduced density. Subsequently, the system was allowed to condense to liquid densities[11] at 450 K over a period of 0.5 ns. A constant temperature and pressure (NPT) trajectory of 0.5 ns was performed to establish the equilibrium density at 450 K. The system was further equilibrated at constant density for about 20 ns (greater than the Rouse time[12] of 15 ns). This was followed by a sampling trajectory of 3 ns. The equilibrated system at 450 K was cooled to 400 K during a 1 ns NPT trajectory. A 6 ns constant density and temperature (NVT) equilibration run was then performed, followed by a 2 ns sampling run. The procedure was repeated for the 298 K system. The equilibrium densities obtained from the simulations for a-PS are 1.051 g/cm^3 (298 K) and 0.995 g/cm^3 (450 K) for the molecular weight considered. The m-DPP and r-DPP systems consisted of 100 molecules each. As with a-PS, these systems were generated on a lattice at greatly reduced density. Following a procedure similar to that described for a-PS, the DPP systems were equilibrated at 450 and 298 K. After 2 ns of equilibration, 1 ns sampling trajectories were performed. Bond lengths were constrained using SHAKE[13] algorithm for all simulations. A cutoff distance of 11 Å and a integration time step of 1 fs were used. NVT conditions were implemented using the Nose−Hoover thermostat and explicit reversible integrators described elsewhere.[12]

III. Results and Discussion

A. Computation of Scattering from Simulation. Scattering experiments measure intensity as a function of the scattering vector q. The scattering intensity can be calculated from simulations through Fourier transforms of the radial distribution functions. Experimentally, after subtracting the self-scattering from the corrected intensity $I_{corr}(q)$, the X-ray structure factor $S(q)$ is obtained:

$$S(q) \propto kI_{corr}(q) - \sum_i f_i^2(q) \qquad (1)$$

where k is a normalization factor for unit conversion, $f_i(q)$ are the atomic form factors, and the sum is carried out over all atoms in the scattering volume. In terms of atomic coordinates, $S(q)$ for polystyrene is given by

$$S(q) = \rho\int_0^\infty [x_C^2 f_C(q)^2 h_{CC}(r) + 2x_C x_H f_C(q) f_H(q) h_{CH}(r) + x_H^2 f_H(q)^2 h_{HH}(r)] \frac{\sin(qr)}{qr} 4\pi r^2 \, dr \qquad (2)$$

where the $h(r)$ functions are net radial distribution functions, $h(r) = g(r) - 1$, where $g(r)$ is a radial distribution function. The functions $f_i(q)$ are obtained from X-ray crystallographic data,[15] the x_i are the number fractions of each atom type, and ρ is the number density of scattering centers (atoms).

B. Comparison with Experiment. In Figure 1, the calculated intensity $I_{corr}(q)$ for a-PS at 298 K is compared with experiment at 293 K.[3] Good agreement for the width and height for the amorphous peak is seen. Simulations do a credible job in reproducing the polymerization peak as well as higher q intramolecular structure. There is a discrepancy in the intensity of the polymerization peak between simulation and experiment that may be due to a number of factors, such as inaccuracies in the potential function, finite system size effects, chain length differences, and the thermal history of the experimental sample. Variation between simulation and experiment is similar to that seen between experiments for different a-PS samples,[2−4] where it is known that the scattering intensity depends on the thermal history of the material.[16] Figure 2 shows the intensity of the polymerization peak and amorphous peak for a-PS relative to the intensity (peak height) at 293 K from experiment[3] and 298 K from simulation as a function of temperature. In agreement with experiment, the simulations show a strong increase in intensity for the polymerization peak with increasing temperature and nearly no temperature dependence for the intensity of the amorphous peak.

C. Comparison of Diphenylpentane Enantiomers and Atactic Polystyrene. The X-ray structure factors (eq 2) from simulation for r-DPP, m-DPP, and a-PS at 298 and 450 K are compared in Figure 3. While benzene and the styrene monomer do not show a polymerization peak, a low-q peak is seen in the polystyrene dimer DPP. Since DPP is certainly not a polymer, and as shown below, the origin of the peak in DPP and a-PS is similar, we believe "polymerization" peak is a misleading name for this feature. Hence, from this point we refer to this feature as the low-q peak and the peak at around 1.1−1.4 Å^{-1} as the high-q peak.

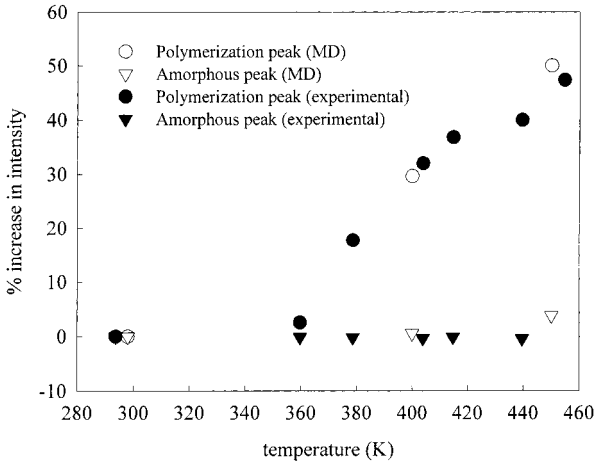

Figure 2. Temperature dependence of relative (to 298 K) intensities of low-q and high-q peaks of atactic polystyrene. Experimental data are from ref 3.

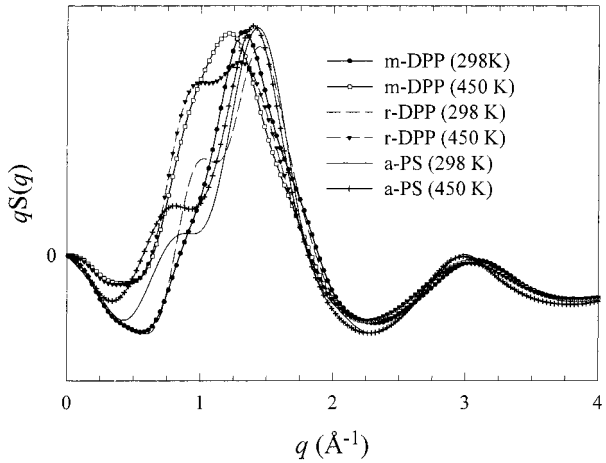

Figure 3. X-ray structure factor for atactic polystyrene, racemic diphenylpentane, and meso diphenylpentane at 298 and 450 K from molecular dynamics simulations.

While the DPP enantiomers have in common with a-PS the presence of the low-q and high-q amorphous features, there are important differences that must be accounted for in any explanation of these features. First, while the low-q feature increases in intensity with increasing temperature in DPP as in a-PS, the feature is shifted to higher q in DPP compared to a-PS and is much stronger in r-DPP compared to m-DPP. Second, the high-q peak in DPP is shifted to lower q compared to a-PS, and both the position and intensity of the peak are dependent upon the enantiomer. Finally, while the peak height for the high-q peak is nearly independent of temperature for both m-DPP and a-PS, the peak decreases sharply with increasing temperature for r-DPP.

D. Scattering in Atactic Polystyrene. Here, we look at the contributions to scattering in a-PS in an effort to understand the structure leading to the low-q and high-q peaks. First, we examine the contributions of phenyl−phenyl, backbone−backbone, and phenyl−backbone scattering to the peaks, as well as their temperature dependence. Then, we investigate intermolecular and intramolecular contributions to the scattering. In the next section, we analyze the DPP enantiomers.

1. Phenyl−Phenyl, Backbone−Backbone, and Phenyl−Backbone Contributions. The phenyl−phenyl, backbone−backbone, and phenyl−backbone contributions to the a-PS structure factor were determined using eq 2, where the sum is restricted to the appropriate (phenyl or backbone) types of carbon and hydrogen atoms. Figure 4 shows the individual contributions as well as the total structure factor for a-PS at 298 and 450 K. From the figure, it is clear that the high-q peak is due mainly to phenyl−phenyl correlations, while the low-q peak is due mainly to backbone−backbone correlations.

Examining the high-q peak in a-PS in detail, it can be seen that the phenyl−phenyl contribution shifts slightly to lower q with increasing temperature and actually increases in intensity while the phenyl−backbone and backbone−backbone correlations, which make relatively minor contributions to the high-q peak, are nearly independent of temperature. None of the individual contributions show behavior with temperature expected of an amorphous halo, i.e., a sharp shift to lower q and decrease in intensity with increasing

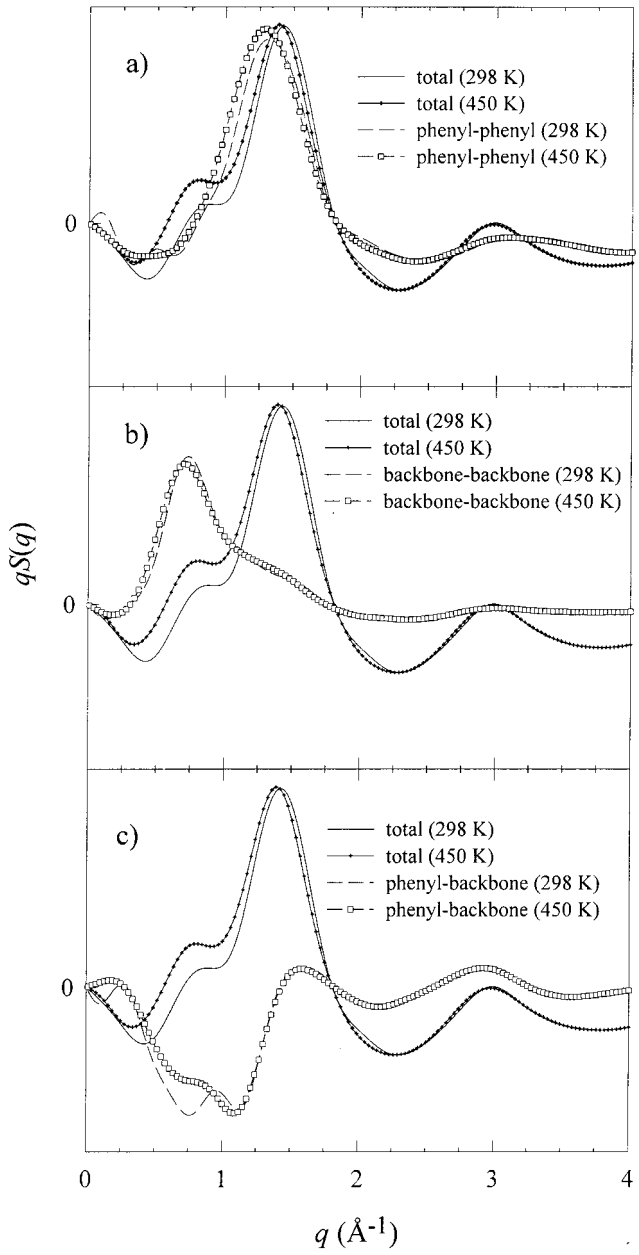

Figure 4. Contributions of phenyl−phenyl, phenyl−backbone, and backbone−backbone correlations to the X-ray structure factor of atactic polystyrene at 298 and 450 K from molecular dynamics simulations.

temperature, leading to the conclusions, supported by the analysis below, that intermolecular correlations alone cannot account for the "amorphous" peak.

Turning to the low-q peak, it can be seen that the "anomalous" temperature dependence of the peak is not due to the temperature dependence of the underlying backbone−backbone correlations which, unlike the amorphous peak, have the expected temperature dependence for an intermolecular peak—a decrease in intensity and shift to lower q with increasing temperature. Rather, it is the temperature dependence of the phenyl−phenyl and phenyl−backbone correlations that lead to an increase in intensity of the low-q peak with increasing temperature. For the phenyl−phenyl correlations, this is a result of a shift of the peak to lower q with increasing temperature, with a consequence that the low-q tail of the correlations contribute more to the low-q peak at higher temperature. The phenyl−backbone

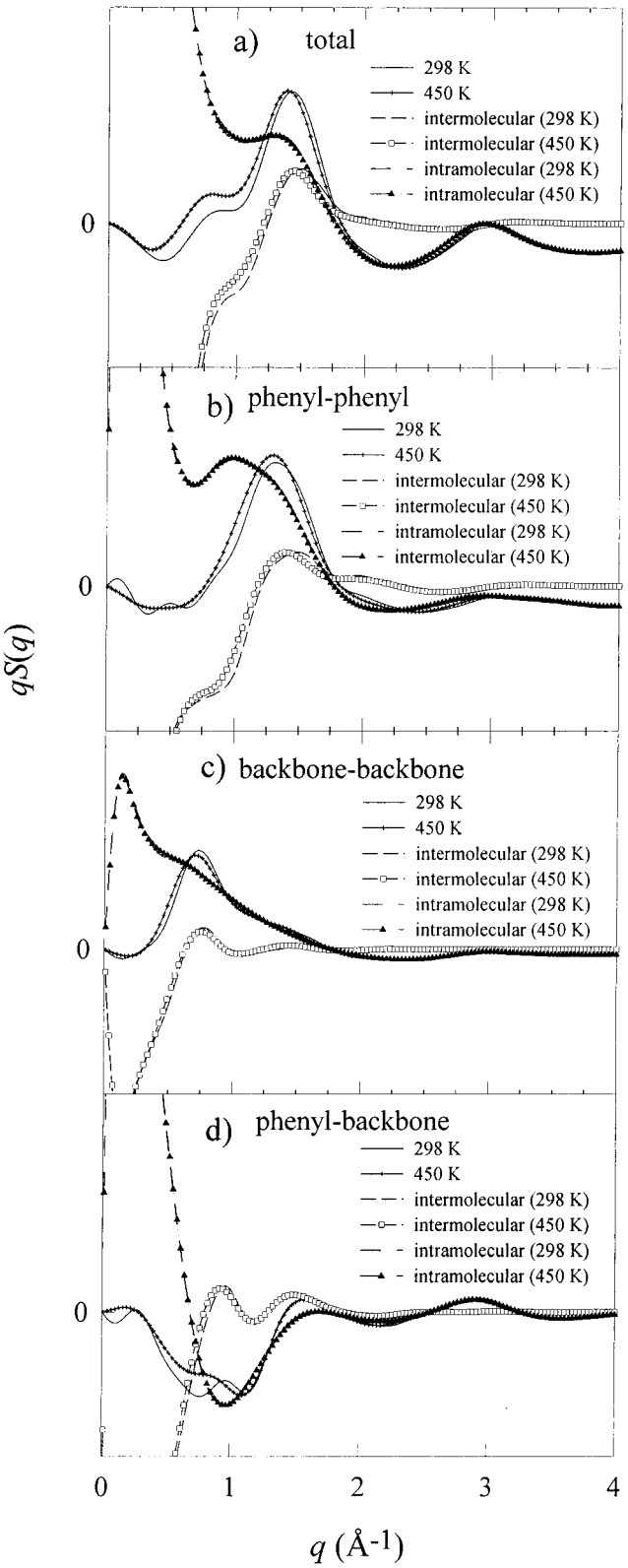

Figure 5. Intramolecular and intermolecular contributions to the total, phenyl−phenyl, phenyl−backbone, and backbone−backbone correlations in atactic polystyrene at 298 and 450 K from molecular dynamics simulations.

contribution to the temperature dependence of the low-q peak is discussed below.

2. Intermolecular and Intramolecular Contributions. In Figure 5, the intramolecular and intermolecular contributions to the X-ray structure factor of a-PS are shown. The intramolecular contributions were determined using eq 2 with $h_{intra}(r) = g_{intra}(r)$, while the intermolecular contributions were determined using eq 2 with $h_{inter}(r) = g_{inter}(r) - 1$. All intrachain correlations were considered to be intramolecular; hence, the intramolecular structure factor corresponds to the single chain structure factor. The intermolecular contribution is calculated by subtracting the intramolecular contribution (obtained from single chain analysis of the polymer melt) from the total interactions, thus taking into account the parent−image interactions in a correct way. It can be seen in Figure 5a that there are important intramolecular and intermolecular contributions to the high-q peak, while structure in the low-q peak region appears to be primarily intermolecular in origin. The intramolecular scattering shows almost no temperature dependence, indicating that changes in the structure factor with temperature are mainly the result of changes in intermolecular correlations. The nearly temperature-independent contribution of intramolecular interactions to the high-q peak accounts for the weak temperature dependence of this peak.

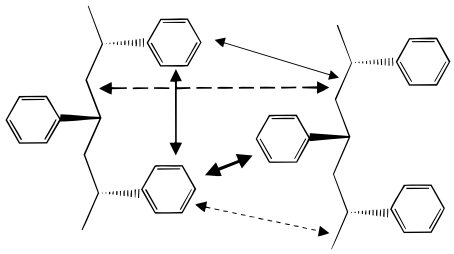

Figure 6. Schematic illustration of various contributions to the low-q (dashed arrow) and high-q (solid arrow) peaks in the X-ray structure factor of atactic polystyrene. Thickness of the arrows represents relative contributions.

Figure 5b−d shows the intramolecular and intermolecular contributions to the individual correlations. Particularly interesting are the contributions to the phenyl−backbone correlations, whose increase with increasing temperature accounts to a large extent for the increase in intensity of the low-q peak (see Figure 4c). The intermolecular contribution the phenyl−backbone correlations shows two peaks at around 1.4 and 0.8 Å^{-1}. The former constitutes the primary contribution of phenyl−backbone correlations to the high-q peak. The latter is due to intermolecular phenyl−backbone correlations that lie spatially between phenyl−phenyl (q = 1.3 Å^{-1}, r = 5.8 Å) correlations and backbone−backbone (q = 0.8 Å^{-1}, r = 9.4 Å) correlations. It is the shift of the *intermolecular* phenyl−backbone and phenyl−phenyl correlations (Figure 5, d and b) to larger distances, and hence smaller q, with increasing temperature that accounts for the temperature dependence of the low-q peak. A schematic illustration of various contributions to the low-q and high-q peaks is shown in Figure 6.

E. Scattering in Diphenylpentane. Simulations reveal that, qualitatively, contributions to the low-q and high-q features in DPP are similar to that seen in a-PS—the high-q feature is due primarily to phenyl−phenyl correlations and the low-q feature to backbone−backbone correlations. The temperature dependence of the low-q feature in the DPP enantiomers is, as in a-PS, due primarily to changes in intermolecular phenyl−phenyl and phenyl−backbone correlations. However, Figure 3 reveals that the high-q feature is shifted to lower q and the low-q feature to higher q in DPP compared to a-PS. This is consistent with a shift in

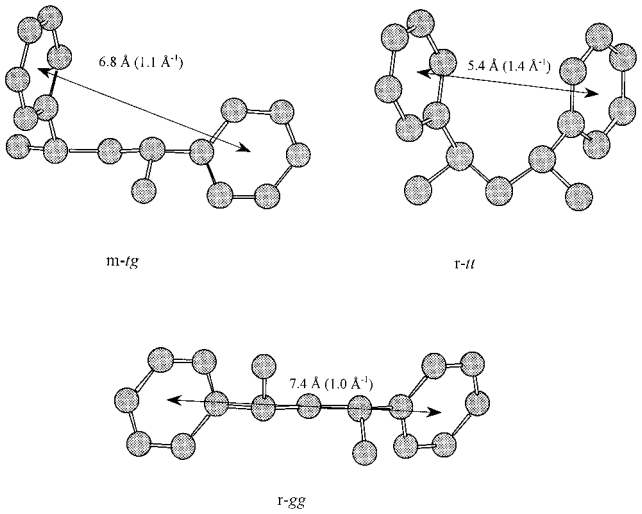

Figure 7. Most important conformations of liquid meso and racemic diphenylpentane. Shown are the distances between the center of mass of the phenyl rings and the (approximate) corresponding q value.

phenyl−phenyl correlations to lower q and backbone−backbone correlations to higher q in DPP compared to a-PS. This difference in phenyl−phenyl correlations is largely intramolecular in origin while the difference in backbone−backbone correlations is primarily intermolecular in origin. The shift of phenyl−phenyl correlations to lower q in DPP is due to the fact that the extended chain structure in a-PS results in more close intramolecular phenyl−phenyl interactions, while the shift of backbone−backbone correlations in DPP to higher q reflects the closer approach of molecular backbones accessible for these short molecules.

We must also account for the much greater intensity for the low-q feature observed in r-DPP compared to m-DPP, the reduced intensity of the high-q peak in r-DPP compared to m-DPP, and the shift in position and greater temperature dependence for the high-q peak in r-DPP compared to m-DPP. Simulations show that the underlying backbone−backbone correlations leading to the low-q feature are very similar for r-DPP and m-DPP. This reflects similar intermolecular packing in r-DPP and m-DPP and is consistent with the nearly identical densities found for the two liquids from simulations. Hence, differences in scattering between r-DPP and m-DPP are not due to differences in backbone correlations. The differences in scattering between r-DPP and m-DPP can be explained by examining the important conformations of these molecules, shown in Figure 7, and the influence of the conformations on phenyl−phenyl and phenyl−backbone correlations.

Experiment reveals that m-DPP is dominantly a single conformer, namely *tg*,[17] while r-DPP is a mixture of two conformers, with the population of the minority *gg* conformer increasing with increasing temperature at the expense of the *tt* conformer.[17] Our simulation results are in agreement with these observations.[18] The difference in structure between r-DPP and m-DPP leads to differences in phenyl−phenyl and phenyl−backbone correlations between the two liquids. In particular, phenyl−phenyl and phenyl−backbone correlations are reduced in the region of 1.1 Å^{-1} (the high-q peak in m-DPP) in r-DPP compared to m-DPP and increased at 0.8 Å^{-1} (low-q feature) and 1.3 Å^{-1} (the high-q peak in r-DPP). These effects, which are primarily intermolecular in origin for the low-q peak region and have both intramolecular and intermolecular contributions in the high-q peak region, account for the higher intensity of the low-q peak in r-DPP, the higher intensity of the high-q peak in m-DPP, and the shift of the high-q peak to higher q in r-DPP. The stronger temperature dependence of the high-q peak in r-DPP is due in part to a reduction in *tt* conformer population, which contributes intramolecularly to scattering at larger q because of close phenyl−phenyl interactions (see Figure 7), with increasing temperature. Note that with increasing temperature the difference between the r-DPP and m-DPP structure factors diminishes (Figure 3), consistent with a reduction in intermolecular correlations due to thermal disorder and a reduction in the population of the *tt* r-DPP population.

IV. Conclusions

Detailed analysis of structure in a-PS and DPP obtained from molecular dynamics simulations reveals that the "polymerization" peak, which is due primarily to intermolecular backbone−backbone correlations, is also present in the dimer. It is further supported by the absence of the peak in styrene and liquid benzene (observed in our simulations), where the above-mentioned correlations are not present. The intermolecular origin of the low-q peak is consistent with experiments on drawn samples. The temperature dependence of the backbone−backbone correlations underlying the low-q peak is that expected of intermolecular correlations in amorphous materials—shift to lower q and a reduction in intensity with increasing temperature. In this sense, the low-q peak reflects interchain packing and is the true amorphous peak in a-PS. The high-q "amorphous" peak is found to be due mainly to phenyl−phenyl correlations, with an important, nearly temperature-independent intramolecular phenyl−phenyl and phenyl−backbone contribution leading to a weak temperature dependence of intensity of the peak, contrary to the behavior of the amorphous halo in most polymers The shift of intermolecular phenyl−backbone and phenyl−phenyl contributions to lower q with increasing temperature leads to the apparent anomalous temperature dependence of the low-q peak, as this peak is the sum of the underlying backbone−backbone correlations and the low-q tail of the phenyl−backbone and phenyl−phenyl correlations. Hence, the "anomalous" temperature dependence of the low-q peak is not indicative of increasing order with increasing temperature.

Acknowledgment. The authors gratefully acknowledge support from ACS-PRF Grant 30333-G7 and NASA Grant NCC-1701 for this work.

References and Notes

(1) Katz, J. R. *Trans. Faraday Soc.* **1936**, *32*, 77.
(2) Schubach, H. R.; Nagy, E.; Heise, B. *Colloid Polym. Sci.* **1981**, *259*, 789.
(3) Mitchell, G. R.; Windle, A. H. *Polymer* **1984**, *25*, 906.
(4) Adams, R.; Balyuzi, H. H.; Burge, R. E. *J. Mater. Sci.* **1972**, *7*, 1249.
(5) Mondello, M.; Yang, H. J.; Furuya, H.; Roe, R. J. *Macromolecules* **1994**, *27*, 3566.
(6) Han, J.; Boyd, R. H. *Polymer* **1996**, *37*, 1797.
(7) Jaffe, R. L.; Smith, G. D. *J. Chem. Phys.* **1996**, *105*, 2780.
(8) Smith, G. D.; Jaffe, R. L. *J. Phys. Chem.* **1996**, *100*, 9624.
(9) Smith, G. D.; Ayyagari, C.; Jaffe, R. L.; Pekny, M.; Bernarbo, A. *J. Phys. Chem. A* **1998**, *102*, 4694.
(10) Gunsteren, W. F.; Berendsen, H. J. C. *Mol. Phys.* **1982**, *45*, 637.

(11) Brandrup, J.; Immergut, E. H.; Grulke, E. A. *Polymer Handbook*; John Wiley and Sons Inc.: New York, 1999.
(12) Doi, M.; Edwards, S. F. *The Theory of Polymer Dynamics*; Oxford University Press: New York, 1986.
(13) Ryckaert, J.; Ciccotti, G.; Berendsen, H. J. C. *J. Comput. Phys.* **1997**, *23*, 327.
(14) Martyna, G. J.; Tuckerman, M. E.; Tobias, D. J.; Klein, M. L. *Mol. Phys.* **1996**, *87*, 1117.
(15) International Union of Crystallography. *International tables for X-ray crystallography*; Kynoch Press: Birmingham, England, 1969.
(16) Kotelyanskii, M.; Wagner, N. J.; Paulaitis, M. E. *Macromolecules* **1996**, *29*, 8497.
(17) Moritani, T.; Fujiwara, Y. *J. Chem. Phys.* **1973**, *59*, 1175.
(18) Ayyagari, C. Molecular Dynamics Simulations of Polystyrene and Its Oligomers. Masters Thesis, University of Utah, 1999.

MA0003553